A new approach to turbulence modeling

By B. Perot[1] AND P. Moin[2]

A new approach to Reynolds averaged turbulence modeling is proposed which has a computational cost comparable to two equation models but a predictive capability approaching that of Reynolds stress transport models. This approach isolates the crucial information contained within the Reynolds stress tensor, and solves transport equations only for these "reduced" variables. In this work, DNS data is used to analyze the nature of these newly proposed turbulence quantities and the source terms which appear in their respective transport equations. The physical relevance of these quantities is discussed and some initial modeling results for turbulent channel flow are presented.

1. Introduction

1.1 Background

Two equation turbulence models, such as the k/ϵ model and its variants are widely used for industrial computations of complex flows. The inadequacies of these models are well known, but they continue to retain favor because they are robust and inexpensive to implement. The primary weakness of standard two equation models is the Boussinesq eddy viscosity hypothesis. This constitutive relationship is rarely applicable in complex flows. Algebraic Reynolds stress models (or non-linear eddy viscosity models) assume a more complex (nonlinear) constitutive relation for the Reynolds stresses. These models are often derived from truncated forms of the full Reynolds stress transport equations. While they can significantly improve the model performance under some conditions, they also tend to be less robust and usually require more iterations to converge (Speziale, 1994). Furthermore, the work of Lund & Novikov suggests that even in their most general form, these models are fundamentally incapable of completely representing the Reynolds stresses. Industrial interest in using full second moment closures (the Reynolds stress transport equations) is hampered by the fact that these equations are much more expensive to compute, converge slowly, and are highly susceptible to instability.

In this work, a turbulence model is explored which does not require the assumption of a constitutive relation for the Reynolds stresses but still is considerably cheaper to compute than standard second moment closures. This alternative approach is made possible by abandoning the Reynolds stresses as the primary turbulence quantity of interest. The Reynolds stresses appear only as a divergence in the

1 Aquasions Inc., Canaan NH

2 Stanford University, Stanford CA

averaged Navier-Stokes equations and therefore contain twice as much information as the mean flow requires. Moving to a minimal set of turbulence variables reduces the overall work by roughly half, but introduces a set of new turbulence variables, which at this time are poorly understood. This project attempts to use DNS data to better understand these new turbulence variables and their exact and modeled transport equations.

1.2 Formulation

The averaged Navier-Stokes equations take the following form for incompressible, constant-property, isothermal flow:

$$\nabla \cdot \mathbf{u} = 0 \tag{1a}$$

$$\frac{\partial \mathbf{u}}{\partial t} + \mathbf{u} \cdot \nabla \mathbf{u} = -\nabla p + \nabla \cdot \nu \mathbf{S} - \nabla \cdot \mathbf{R} \tag{1b}$$

where $\mathbf{u}$ is the mean velocity, p is the mean pressure, ν is the kinematic viscosity, $\mathbf{S} = \nabla \mathbf{u} + (\nabla \mathbf{u})^T$ is twice the rate-of-strain tensor, and $\mathbf{R}$ is the Reynolds stress tensor. The evolution of the Reynolds stress tensor is given by:

$$\frac{\partial \mathbf{R}}{\partial t} + \mathbf{u} \cdot \nabla \mathbf{R} = \nabla \cdot \nu \nabla \mathbf{R} + \mathbf{P} - \boldsymbol{\epsilon} + \mathbf{\Pi} - \nabla \cdot \mathbf{T} - [\nabla \mathbf{q} + (\nabla \mathbf{q})] \tag{2}$$

where $\mathbf{P}$ is the production term, $\boldsymbol{\epsilon}$ is the (homogeneous) dissipation rate tensor, $\mathbf{\Pi}$ is the pressure-strain tensor, $\mathbf{T}$ is the velocity triple-correlation, and $\mathbf{q}$ is the velocity-pressure correlation. The last four source terms on the right-hand side must be modeled in order to close the system. The production term $\mathbf{P}$ is exactly representable in terms of the Reynolds stresses and the mean velocity gradients. This is the standard description of the source terms, but it is by no means unique and there are numerous other arrangements.

Note that turbulence effects in the mean momentum equation can be represented by a body force $\mathbf{f} = \nabla \cdot \mathbf{R}$. One could construct transport equations for this body force (which has been suggested by Wu *et al.*, 1996) but mean momentum would no longer be conserved. To guarantee momentum conservation, the body force is decomposed using Helmholtz decomposition, into its solenodal and dilatational parts, $\mathbf{f} = \nabla \phi + \nabla \times \boldsymbol{\psi}$. A constraint (or gauge) must be imposed on $\boldsymbol{\psi}$ to make the decomposition unique. In this work we take $\nabla \cdot \boldsymbol{\psi} = 0$. With this choice of gauge, the relationship between ϕ and $\boldsymbol{\psi}$ and the Reynolds stress tensor is given by,

$$\nabla^2 \phi = \nabla cdot (\nabla \cdot \mathbf{R}) \tag{3a}$$

$$\nabla^2 \boldsymbol{\psi} = -\nabla times (\nabla \cdot \mathbf{R}) \tag{3b}$$

Note that the choice of gauge influences the value of $\boldsymbol{\psi}$, but not the effect that $\boldsymbol{\psi}$ has on the mean flow.

Using these relationships, transport equations for ϕ and $\boldsymbol{\psi}$ can be derived from the Reynolds stress transport equations.

$$\frac{\partial \phi}{\partial t} + \mathbf{u} \cdot \nabla \phi = \nu \nabla^2 \phi - 2\nabla \cdot \mathbf{q} - \nabla^{-2} \nabla \cdot \nabla \cdot [\boldsymbol{\epsilon} - \mathbf{\Pi} + \nabla \cdot \mathbf{T} - \mathbf{P} + \mathbf{S}_\phi] \tag{4a}$$

$$\frac{\partial \boldsymbol{\psi}}{\partial t} + \mathbf{u} \cdot \nabla \boldsymbol{\psi} = \nu \nabla^2 \boldsymbol{\psi} + \nabla \times \mathbf{q} + \nabla^{-2} \nabla \times \nabla \cdot [\boldsymbol{\epsilon} - \boldsymbol{\Pi} + \nabla \cdot \mathbf{T} - \mathbf{P} + \mathbf{S}_\psi] \qquad (4b)$$

These equations contain extra production-like source terms $\mathbf{S}_\phi$ and $\mathbf{S}_\psi$ which contain mean velocity gradients. Note that the production term is not an explicit function of ϕ and $\boldsymbol{\psi}$ (except under limited circumstances) and, in general, must now be modeled.

2. Theoretical Analysis

2.1 Turbulent Pressure

Taking the divergence of Eqn. 1a (the mean momentum equation) gives the classic Poisson equation for pressure,

$$\nabla^2 p = -\nabla \cdot (\mathbf{u} \cdot \nabla \mathbf{u}) - \nabla \cdot (\nabla \cdot \mathbf{R}) \qquad (5)$$

Since this is a linear equation, the pressure can be conceptually split into two terms, and one can think of the mean pressure as being a product of a mean flow pressure due to the first term on the right-hand side,

$$\nabla^2 P_{mean} = -\nabla \cdot (\mathbf{u} \cdot \nabla \mathbf{u}) \qquad (6a)$$

and a turbulent pressure due to the second term on the right-hand side.

$$\nabla^2 P_{turb} = -\nabla \cdot (\nabla \cdot \mathbf{R}) \qquad (6b)$$

Given the definition of ϕ and assuming that ϕ is zero when there is no turbulence (which is the intuitive boundary condition) then it is clear that $\phi = -P_{turb}$. For this reason, ϕ will be referred to as the turbulent pressure. This quantity is added to the mean pressure in the averaged momentum equation, which results in P_{mean} being the effective pressure for the averaged equations. The mean flow pressure. P_{mean} tends to vary more smoothly than p which aids the numerical solution of these equations.

For turbulent flows with a single inhomogeneous direction the turbulent pressure can be directly related to the Reynolds stresses. In this limit, Eqn. 3a becomes, $\phi_{22} = R_{22,22}$ where x_2 is the direction of inhomogeneity. This indicates that $\phi = R_{22}$ for these types of flows. Note that $R_2 2$ is positive semi-definite, so the turbulent pressure is always greater than or equal to zero in this situation. Positive turbulent pressure is consistent with the picture of turbulence as a collection of random vortices (with lower pressure cores) embedded in the mean flow. It is not clear what the conditions for a negative turbulent pressure would be, if this condition is indeed possible.

2.2 Turbulent Vorticity

To understand the role of $\boldsymbol{\psi}$ it is instructive to look again at turbulent flows that have a single inhomogeneous direction. Under this restriction Eqn. 3b becomes $\psi_{i,22} = -\epsilon_{i2k} R_{k2,22}$ where x_2 is the direction of inhomogeneity. If $\boldsymbol{\psi}$ goes to zero

when there is no turbulence (the intuitive boundary condition) then $\psi_i = -\epsilon_{i2k}R_{k2}$, or $\psi_1 = -R_{32}$, $psi_2 = 0$ and $\psi_3 = R_{12}$. These are the off diagonal, or shear stress components of the Reynolds stress tensor.

For two-dimensional mean flows (with two inhomogeneous flow directions), only the third component of $\boldsymbol{\psi}$ is non-zero and Eqn. 3b becomes

$$\psi_{3,11} + \psi 3,22 = R_{12,22} - R_{12,11} + (R_{11} - R_{22})_{12} \tag{6}$$

Since $\boldsymbol{\psi}$ is responsible for vorticity generation it is appropriate that it be aligned with the vorticity in two dimensional flows. As a first level of approximation, it is not unreasonable to think of $\boldsymbol{\psi}$ as representing the average vorticity of a collection of random vortices making up the turbulence, and it is reasonable to consider $\boldsymbol{\psi}$ as the turbulent vorticity.

2.3 Relationship with the Eddy Viscosity Hypothesis

Despite the shortcomings of the linear (Boussinesq) eddy viscosity hypothesis, it is clearly a good first approximation of turbulence effects. The linear eddy viscosity hypothesis for incompressible flows takes the form,

$$\mathbf{R} = -\nu_T(\nabla\mathbf{u} + (\nabla\mathbf{u})^T) + \frac{2}{3}k\mathbf{I} \tag{7}$$

where ν_T is the eddy viscosity, $\mathbf{I}$ is the identity matrix, and k is one half the trace of the Reynolds stress tensor.

Taking the divergence of Eqn. 7 and rearranging terms gives,

$$\mathbf{f} = -\nabla \cdot \mathbf{R} = \nabla(-\frac{2}{3}k + 2\mathbf{u} \cdot \nabla\nu_T) - \nabla \times (\nu_T\nabla \times \mathbf{u}) - 2\mathbf{u} \cdot \nabla(\nabla\nu_T). \tag{8}$$

If the eddy viscosity varies relatively slowly, as is usually the case, then the very last term (involving the second derivative of the eddy viscosity) will be small and can be neglected. Under these circumstances the linear eddy viscosity model is equivalent to the following model,

$$\phi = \frac{2}{3}k - 2\mathbf{u} \cdot \nabla\nu_T \tag{9a}$$

$$\boldsymbol{\psi} = \nu_T\nabla \times \mathbf{u}. \tag{9b}$$

So to a first approximation the turbulent vorticity, $\boldsymbol{\psi}$ should be roughly equal to the resolved vorticity, times a positive eddy viscosity; and the turbulent pressure should be roughly equal to (2/3) of the turbulent kinetic energy. These results are entirely consistent with the findings of the previous subsections.

3. Computational Results

Equations 3a and 3b, relating the turbulent pressure and turbulent vorticity to the Reynolds stresses, were used to calculate ϕ and $\boldsymbol{\psi}$ from DNS data for two relatively complex two-dimensional turbulent flows: a separating boundary layer (Na & Moin) and flow over a backward facing step (Le & Moin). The purpose was to assess the behavior of these new turbulence quantities in practical turbulent situations, and to provide a database of these quantities for later comparison with turbulence models.
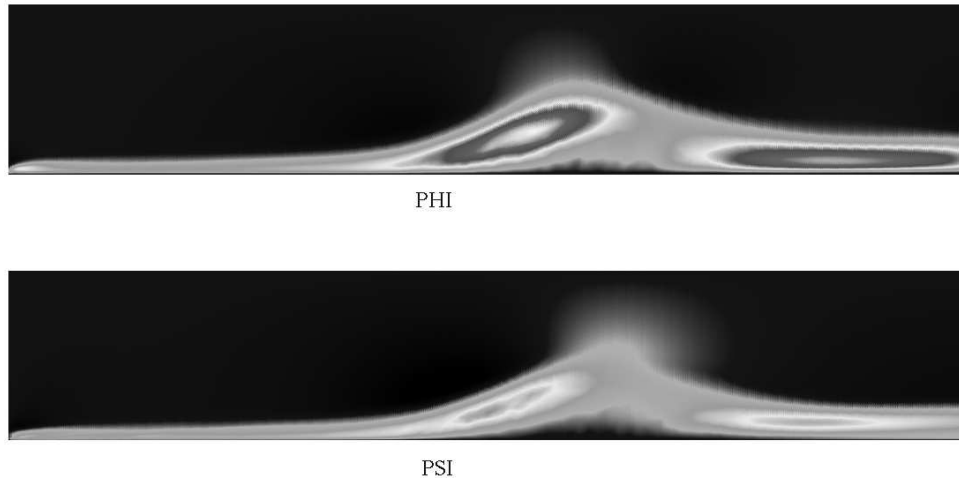
Separated Boundary Layer

PHI

PSI

FIGURE 1. Contours of turbulent pressure (ϕ) and turbulent vorticity ($-\boldsymbol{\psi}$) for the separating boundary layer of Na & Moin.

3.1 Separated Boundary Layer

The values of ϕ and $-\psi_3$ are shown in Figure 1. As mentioned previously, for two dimensional flows only the third component of $\boldsymbol{\psi}$ is nonzero. The flow moves from left to right, separates just before the midpoint of the computational domain, and then reattaches before the exit. The contours are the same for both quantities and range from $-.004U_\infty^2$ to $.01U_\infty^2$, where U_∞ is the inlet free-stream velocity.

Both the turbulent pressure and turbulent vorticity magnitude increase in the separating shear layer and the reattachment zone. In addition, both quantities become slightly negative in the region just in front (to the left) of the separating shear layer, and show some "elliptic" (long range decay) effects at the top of the separation bubble. There is some speculation, at this time, that these effects could be numerical, but there is also some reason to believe that they are a legitimate result of the elliptic (but order one) operators which define these variables. Changes in the far-field boundary condition had little effect on the computed values of ϕ and ψ_3.

The visual observation that ϕ and $-\psi_3$ are roughly proportional, is analogous to the observation that $0.3k \approx R_{12}$ (originally developed by Townsend, 1956, and successfully used in the turbulence model of Bradshaw & Ferriss). It is also consistent with the (first order) notion of turbulence as a collection of embedded vortices, with $-\phi$ representing the average vortex core pressure and $\boldsymbol{\psi}$ representing the average vortex strength.

In the case of a single inhomogeneous direction $-\phi = R_{22}$ and $\psi_3 = -R_{12}$. It is instructive therefore to compare the results shown in Figure 1 with the R_{22} and
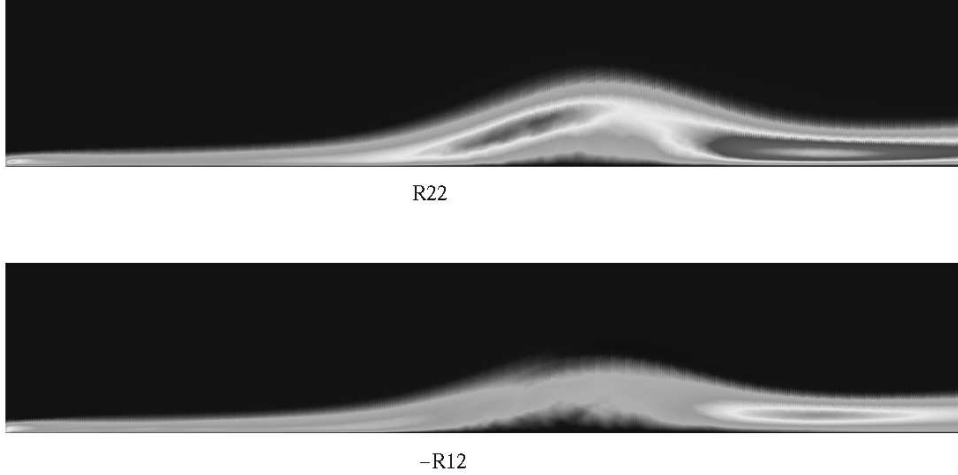
Separated Boundary Layer

R22

−R12

FIGURE 2.   Contours of the normal Reynolds stress (R_{22}) and negative turbulent shear stress ($-R_{12}$) for the separating boundary layer of Na & Moin.

$-R_{12}$ components of the Reynolds stress tensor, shown in Figure 2. The magnitudes of the contours in Figure 2. are the same as Figure 1. This comparison clearly shows the additional effects that result from inhomogeneity in the streamwise direction. The leading and trailing boundary layers (which have very little streamwise inhomogeneity) are almost identical. However, the magnitudes of the turbulent pressure and turbulent vorticity component are enhanced in the separated shear layer due to the streamwise inhomogeneity.

3.2 Backward Facing Step

Computations of ϕ and $-\psi_3$ for the backward facing step are shown in Figure 3. The flow is from left to right, and there is an initial (unphysical) transient at the inflow as the inflow boundary condition becomes Navier-Stokes turbulence. The boundary layer leading up to the backstep has moderate levels of the turbulent pressure and turbulent vorticity (which closely agree with the values of R_{22} and $-R_{12}$ in that region. As with the separating boundary layer, the turbulent pressure and turbulent vorticity increase significantly in the separated shear layer and reattachment zone. There is an area of slight positive turbulent pressure and negative turbulent vorticity in the far field (about one step height) above the backstep corner. This may or may not be a numerical artifact, and is discussed in the next section.

3.3 Ellipticity

Identifying the exact nature of the ellipticity of these new turbulence quantities is important to understanding their overall behavior, and how they should be modeled.
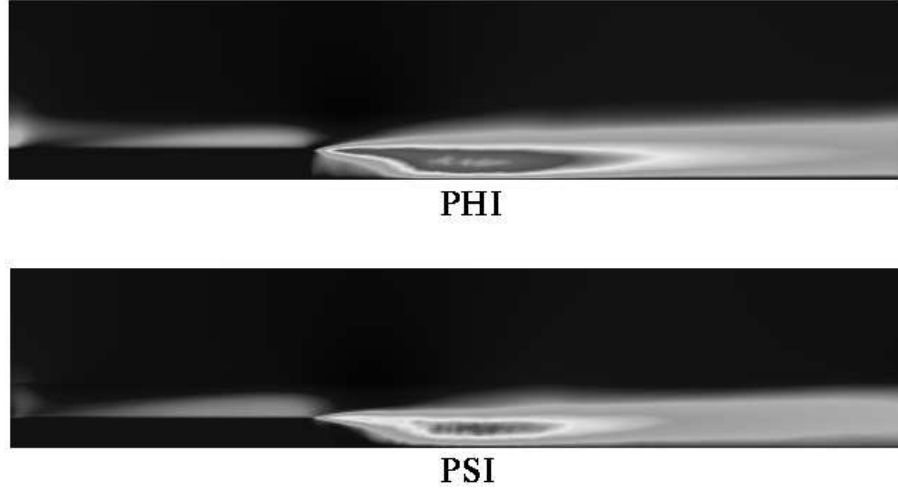
Backward Facing Step

PHI

PSI

FIGURE 3.   Contours of turbulent pressure $(-\phi)$ and turbulent vorticity (ψ) for the backward facing step of Le & Moin.

Rewritten, equations 3a and 3b become,

$$\phi = \nabla^{-2}\nabla cdot(\nabla \cdot \mathbf{R}) \tag{9a}$$

$$\psi = -\nabla^{-2}\nabla times(\nabla \cdot \mathbf{R}) \tag{9b}$$

These are elliptic, but order one, operators on the Reynolds stress tensor. As demonstrated in section 3, when there is only a single inhomogeneous direction, these operators simply select various Reynolds stress components. Under these conditions they do not produce "action at a distance" or long range effects normally associated with elliptic (Poission or Helmholtz) operators.

For two and three inhomogeneous directions, it is still not clear whether these operators produce long range effects. There are certainly some situations in which they do not. One example is if the Reynolds stress tensor can be represented in the following form (somewhat reminiscent of the linear eddy viscosity relation) $R_{ij} = s\delta_{ij} + v_{i,j} + v_{j,i}$, where s is some scalar and $\mathbf{v}$ is a vector. If this is the case then, $\phi = s + 2\nabla \cdot \mathbf{v}$ and $\psi = -\nabla \times \mathbf{v}$, and there are no long range ("elliptic") effects.

In fact, the presence of long range effects in ϕ and ψ is somewhat unsettling. It would suggest that these turbulence quantities can exist in regions where there is no Reynolds stress. Since $\nabla \cdot \mathbf{R} = \nabla\phi + \nabla \times \psi$, this would imply that some sort of complex cancellation of these long range effects must take place when the Reynolds stresses (turbulence) are small or negligible. While the results presented in Figure 1 and 3 can be explained by assuming that elliptic effects must take place, they could also be a numerical artifact. The numerical solution of equations 9a and
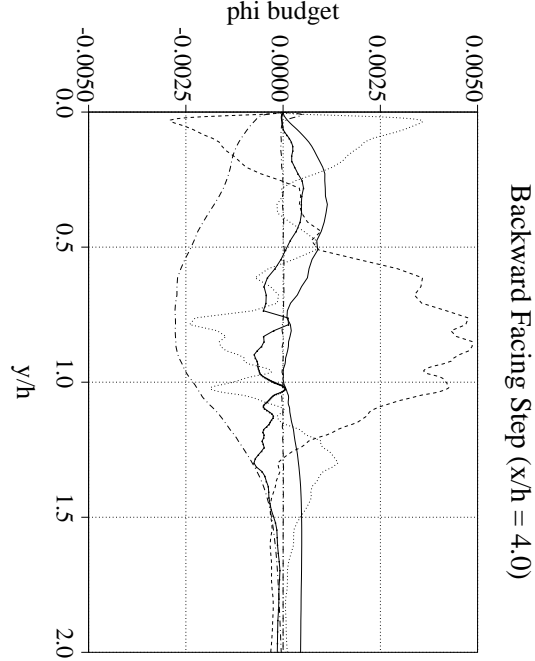
FIGURE 4.   Budget of the ϕ transport equation at a station roughly half way through the recirculation bubble of the backward facing step. —·— , dissipation or diffusion; ---- , velocity pressure-gradient; ········ , triple correlation term; ——— , production or convection.

9b requires double differentiation of numerical data, and results in highly compact Poission equation source terms which are only marginally resolved by the mesh.

It is our current conjecture that these operators are actually local in nature and only serve to "mix" various components of the Reynolds stress tensor. It is also conjectured from these computational results that the turbulent pressure is a positive semi-definite quantity.

3.4 Turbulent Pressure Evolution

Considerable intuition can be obtained about the evolution of the turbulent pressure by considering the case of a single inhomogeneous direction. It has been shown that under these circumstances $\phi = R_{22}$, so the evolution is identical with the Reynolds stress transport equation for the normal Reynolds stress, R_{22}. For the case of turbulent channel flow (Mansour *et al.*), the R_{22} evolution is dominated by a balance between dissipation and pressure-strain, with somewhat smaller contributions from turbulent transport and viscous diffusion. There is considerable interest in determining if these same trends continue for ϕ evolution in more complex situations, since the ultimate goal is to construct a modeled evolution equation for this quantity.

Figure 4. shows the terms in the exact ϕ evolution equation for flow over a backward facing step, at a station roughly in the middle of the recirculation bubble. These terms were reconstructed in the same manner as the turbulent pressure was calculated. Both the detached shear layer and the backwards moving boundary
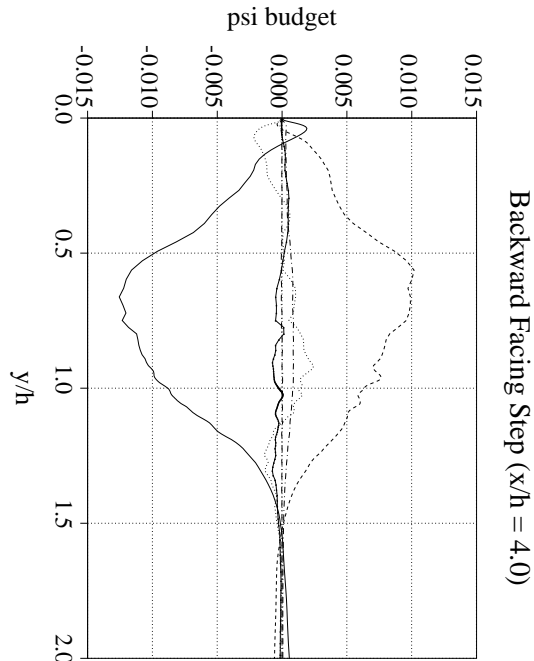
FIGURE 5.   Budget of the ψ_3 transport equation at a station roughly half way through the recirculation bubble of the backward facing step. See Figure 4 for caption.

layer are visible in the statistics. In the shear layer, the expected dominance of dissipation and pressure-terms (presumably dominated by pressure-strain) is present. In the recirculating boundary layer, turbulent transport and pressure-terms (probably dominated by pressure transport) are dominant. It is interesting to note that the production term dominates in the middle of the recirculation bubble. The fact that these source terms do not approach zero at roughly two step heights away from the bottom wall, is thought to be a numerical artifact similar to those found when calculating ϕ and ψ. Some of the curves have an erratic nature due to the lack of statistical samples. This phenomena is also present in the (unsmoothed) Reynolds stress transport equation budgets presented in Le & Moin.

3.5 Turbulent Vorticity Evolution

As with the turbulent pressure, it is useful to consider the case of a single inhomogeneous direction, when analyzing the evolution of the turbulent vorticity. Under these circumstances ψ_3 evolves identically to the Reynolds shear stress, R_{12}. In turbulent channel flow, the R_{12} evolution is dominated by a balance between production and pressure-strain, with somewhat smaller contributions from turbulent and pressure transport. This trend continues in the ψ_3 evolution equation, which is shown in Figure 5., for the backward facing step at a cross section roughly halfway through the recirculization bubble. The small value of the dissipation is consistent with the fact that isotropic source terms can be shown not contribute to the evolution of ψ.

4. Modeling

4.1 Formulation

The proposed transport equations for the turbulent pressure and turbulent vorticity are,

$$\frac{\partial \phi}{\partial t} + \mathbf{u} \cdot \nabla \phi = \nu \nabla \cdot (\nu + \nu_T) \nabla \phi - (\frac{3}{2} C_\mu)(\frac{1}{T})\phi - (\frac{12\nu}{y^2})\phi + (\frac{2}{3})\frac{\boldsymbol{\psi} \cdot \boldsymbol{\psi}}{15\nu + \nu_T} \quad (10a)$$

$$\frac{\partial \boldsymbol{\psi}}{\partial t} + \mathbf{u} \cdot \nabla \boldsymbol{\psi} = \nu \nabla \cdot (\nu + \nu_T) \nabla \boldsymbol{\psi} - (\frac{1}{T})\boldsymbol{\psi} - (\frac{6\nu}{y^2})\boldsymbol{\psi} + \phi \boldsymbol{\omega} \quad (10b)$$

where $C_\mu = 0.09$, y is the normal distance to the wall, the inverse timescale is given by $\frac{1}{T} = \frac{\phi}{\nu + \nu_T}$, and the eddy viscosity is given by $\nu_T = \frac{|\boldsymbol{\psi}|}{|\omega|}$. Dissipation (and some redistribution) is modeled as an exponential decay process (roughly corresponding to the Rotta, low Reynolds number dissipation model). Turbulent and pressure transport are collectively modeled as enhanced diffusive transport. Production and energy redistribution are proportional to the turbulence scale times the mean vorticity for the turbulent vorticity, and are proportional to the square of the turbulent vorticity magnitude for the turbulent pressure. High Reynolds number constants are determined so that $\phi = \frac{2}{3}k$ at high Reynolds numbers. Low Reynolds number constants (which appear with a ν) are set to obtain good agreement with the channel flow simulations of the next section.

Note that both ϕ and $\boldsymbol{\psi}$ have the same units. An extra turbulent scale is currently defined by using the mean flow timescale $|\omega|$ to define the eddy viscosity. The solution of an additional scale transport equation (such as ϵ) would remedy a number of potential problems with the current model. It could eliminate the singularity in the eddy viscosity at zero vorticity, remove any explicit references to the wall normal distance, and allow better decay rates for homogeneous isotropic turbulence. The disadvantage of this approach (which will be tested in the future) is the added computational cost and additional empiricism.

4.2 Channel Flow Simulations

The model equations (10a and 10b) were solved in conjunction with mean flow equations for fully developed channel flow at Re_τ of 180 and 395. Since there is only one inhomogeneous direction, the turbulent pressure is proportional to the normal Reynolds stress, and ψ_3 is proportional to the turbulent shear stress. Comparisons of the model predictions and the DNS data of Kim, Moin, & Moser, are shown in Figure 6. Given the initial state of the model, the predictions are surprisingly good.

When a turbulent channel flow is suddenly perturbed by a spanwise pressure gradient, the flow suddenly becomes three dimensional and the turbulence intensities first drop, before increasing due to the increased total shear (Moin *et al.*). Durbin modeled this effect by adding a term to the dissipation equation which increases the dissipation in these three-dimensional flows. The same qualitative effect can be obtained by defining the eddy viscosity in the proposed model as $\nu_T = \frac{\boldsymbol{\psi} \cdot \omega}{\omega cdot \omega}$.
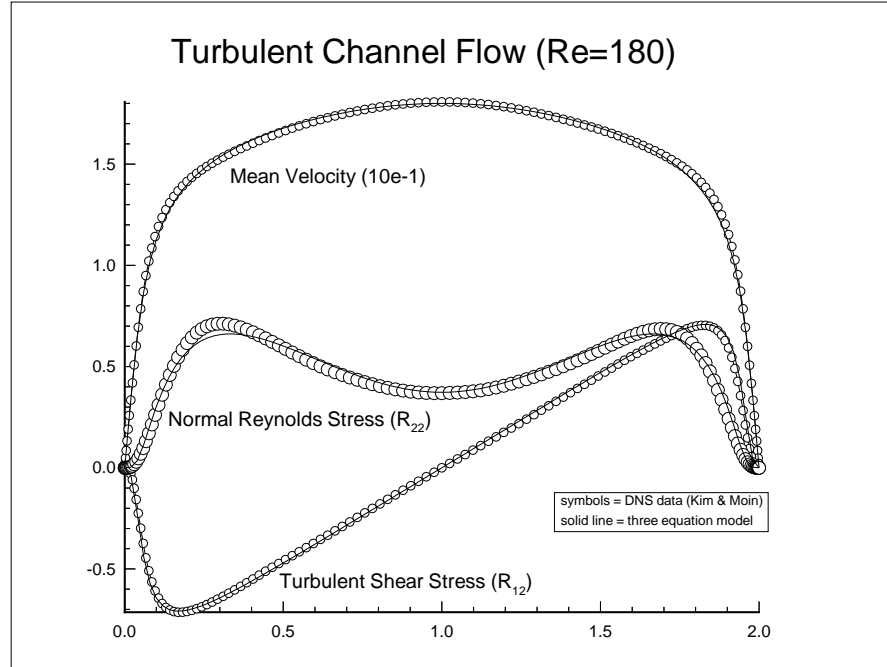
FIGURE 6. Model results (solid lines) and DNS data (circles) for turbulent channel flow. ($Re_\tau = 180$)

In two dimensional flows this is identical to the previous definition. However, in three dimensional flows, the orientation of ψ will lag $\cdot\omega$, and the eddy viscosity will drop initially. A smaller eddy viscosity leads to a smaller timescale and increased dissipation. Unfortunately, the magnitude of this effect is severely underestimated, and a scale equation (and a correction like Durbin's) may be required to model this effect accurately.

5. Conclusions

This work proposes abandoning the Reynolds stresses as primary turbulence quantities, in favor of a reduced set of turbulence variables, namely the turbulent pressure, ϕ, and the turbulent vorticity ψ. The advantage of moving to these alternative variables is the ability to simulate turbulent flows with the accuracy of a Reynolds stress transport model (i.e. with no assumed constitutive relations), but at a significantly reduced cost and simplified model complexity. As the names imply, these quantities are not simply mathematical constructs formulated to replace the Reynolds stress tensor. They are physically relevant quantities. Not only has a new modeling framework been proposed, but in the process we have uncovered an alternative method for qualitatively describing turbulent flows.

At first glance the operators which relate ϕ and ψ to the Reynolds stress tensor suggest the possibility of ellipticity or action at a distance. However, we have shown that under a number of different circumstances this does not happen, and conjecture that it may never happen. The physical relevance of these quantities would be complicated if they were finite when there was no turbulence (Reynolds

stresses). A proof to this effect may also prove our second conjecture, that ϕ is a positive definite quantity.

The budgets for the transport equations of these new variables indicated that the extra production terms were not significant, and that these equations could be modeled analogously to the Reynolds stress transport equations. An initial model was constructed for these equations using very basic modeling constructs which showed good results for turbulent channel flow. It is likely, that for this shearing flow, the turbulent timescale is well represented by the mean flow vorticity. However, for more complex situations, it is likely that an additional scale equation (such as an ϵ equation) will be required.

REFERENCES

BRADSHAW, P. & FERRISS, D.H. 1971 . *J. Fluid Mech..* **46,** 83-110.

DURBIN, P.A. 1993 Modeling three-dimensional turbulent wall layers . *Phys. Fluids A.* **5(5),** 1231-1238.

KIM, J., MOIN, P. & MOSER, R.D. 1987 Turbulence statistics in fully-developed channel flow at low Reynolds number . *J. Fluid Mech..* **177,** 133-166.

LE, H. & MOIN, P. 1995

T. S. LUND, T.S. & NOVIKOV, E.A. 1992 Parameterization of subgrid-scale stress by the velocity gradient tensor . *Annual Research Briefs - 1992.* Center for Turbulence Research, Stanford Univ.

MANSOUR, N.N., KIM, J. & MOIN, P. 1988 Reynolds-stress and dissipation rate budgets in a turbulent channel flow . *J. Fluid Mech..* **194,** 15-44.

MOIN, P., SHIH, T.-H., DRIVER, D. & MANSOUR, N.N. 1990 Direct numerical simulation of a three-dimensional turbulent boundary layer . *Phys. Fluids A.* **2(10),** 1846-1853

NA, Y. & MOIN, P. 1996

ROTTA, J. 1951 Statistical theory of inhomogeneous turbulence. Part I. . *Zeitschrift fur Physik.* **129,** 257-272.

SPEZIALE, C.G. 1994 A review of Reynolds stress models for turbulent flows, . *20th Symposium on Naval Hydrodynamics.* University of California, Santa Barbara

TOWNSEND, A.A. 1956 *The Structure of Turbulent Shear Flow.* Cambridge University Press, London.

WU, J.-Z., ZHOU, Y. & WU, J.-M. 1996 Reduced stress tensor and dissipation and the transport of Lamb vector . *ICASE report.* No. 96-21.